Journal of Power Sources 491 (2021) 229562

Contents lists available at ScienceDirect

Journal of Power Sources

journal homepage: www.elsevier.com/locate/jpowsour

Insight into cathode microstructure effect on the performance of molten carbonate fuel cell

Samih Haj Ibrahim [a,*], Tomasz Wejrzanowski [a,**], Pawel Sobczak [a], Karol Cwieka [a], Aleksandra Lysik [a], Jakub Skibinski [a], Graeme John Oliver [b]

[a] Faculty of Materials Science and Engineering, Warsaw University of Technology, Woloska 141, 02-507, Warsaw, Poland
[b] Cape Peninsula University of Technology, PO Box 1906, Bellville, 7535, South Africa

HIGHLIGHTS

- X-ray tomography was used to create numerical models of the cathode material.
- Molten carbonate electrolyte capillary action in porous cathodes was simulated.
- Cell performance is correlated with surface area of the gas/electrolyte interface.
- Reaction in a thin electrolyte film contributes to improvement of cell performance.

ARTICLE INFO

Keywords:
Capillary infiltration
Molten carbonate fuel cell
Open-porous microstructure
Volume of fluid modeling

ABSTRACT

This paper deals with the effect of pore size distribution within the cathode on the performance of molten carbonate fuel cells. The X-ray tomography images of four materials are used to create 3D geometrical models of the cathodes pore structure so that the modeling takes into account the actual variations in pore size of the real materials. The simulation includes the cathode infiltration process by the liquid electrolyte which is governed by capillary action. This allows one to quantify the triple phase boundary (cathode/electrolyte/gas) density which is commonly viewed as providing active sites for cathodic reactions. It has been found that this parameter does not correlate well with the maximum power density of the cell. On the other hand, increasing the specific surface area of the gas/electrolyte interface correlates well with higher cell performance. Following our in-depth modeling and analysis we postulate that the dominant mechanism, when larger pores are introduced by the addition of porogens, is the creation of continuous pathways for the transport of gases to come into contact with the cathode surface through the thin film of electrolyte.

1. Introduction

Molten Carbonate Fuel Cells (MCFCs) and Solid Oxide Fuel Cells (SOFCs) are the most rapidly developing high temperature fuel cell technologies. They offer promising solutions to reduce the environmental impact of energy production, as they provide the opportunity to generate electricity without emitting harmful substances such as CO_2 into the atmosphere [1]. MCFCs, with a high operating temperature of 650 °C and the possibility of using a variety of fuels such as hydrogen or natural gas, are of particular interest for tri-generation systems such as combined heat and power (CHP) or combined cooling heat and power (CCHP) applications [1–4]. Fuel cells of this type generate power through the conversion of the chemical energy of a gaseous fuel into electricity in electrochemical reactions [2]. Unlike all other types of fuel cells, a MCFC operates with a liquid electrolyte, which is held in porous cell elements by capillary action. Due to that, porosity and in particular pore size is of key importance for the optimization of the spatial distribution of electrolyte and the formation of active sites for catalytic reactions taking place at triple phase boundaries (gas/electrolyte/electrode), TPB, or the electrolyte/electrode interface.

The cathode and anode are porous sinters, facilitating the transport of reactants and the removal of products, while offering a large

* Corresponding author.
** Corresponding author.
E-mail addresses: Samih.ibrahim.dokt@pw.edu.pl (S. Haj Ibrahim), Tomasz.Wejrzanowski@pw.edu.pl (T. Wejrzanowski).

https://doi.org/10.1016/j.jpowsour.2021.229562
Received 8 October 2020; Received in revised form 23 December 2020; Accepted 25 January 2021
Available online 5 February 2021

geometric surface area or density of active sites for chemical reactions. The microstructure and chemical composition of the electrodes should be designed to ensure a strong interaction between the mass transport and catalytic properties, regulating the physio-chemical phenomena [5,6].

Electrode materials should have high electrical conductivity and stability at elevated temperatures in the electrolyte environment. The material commonly used for electrodes is nickel. On the cathode side it is oxidized in situ during the start-up process of the cell, while on the anode it remains in metallic form. The electrodes are separated by a matrix filled with electrolyte. The matrix is a porous γ-lithium aluminate structure with a pore size significantly smaller than the electrodes, which maintains the electrolyte by the action of capillary forces. The electrolyte is an eutectic mixture of lithium and potassium carbonates resulting in ionic conductivity and wettability of the electrodes [2,7].

The principle of operation is that the MCFC generates power by means of electrochemical reactions occurring over the electrodes (anode and cathode). During the work of the cell the conversion of the chemical energy of fuel (hydrogen) and oxidants (oxygen and carbon dioxide) into the electrical energy takes place. The cathode catalyzes the reaction between oxygen (O_2) and carbon dioxide (CO_2) towards the formation of carbonate ions (CO_3^{2-}) as shown below:

$$0.5O_2 + CO_2 + 2e^- \rightarrow CO_3^{2-}$$

These carbonate ions are transported through the electrolyte melt toward the anode where it oxidizes the fuel (hydrogen) and produce free electrons [2]:

$$H_2 + CO_3^{2-} \rightarrow CO_2 + 2e^-$$

The cathode reaction is commonly considered more complex and slower than the anode reaction due to oxygen reduction being regarded as a rate determining step [8–10]. The literature describes mechanisms engaging active forms of oxygen, peroxide and superoxide, produced over the cathode catalyst at triple phase boundaries (between electrode, molten electrolyte and gases) [11–13]. As a complementary mechanism, the formation of carbonate ions at the boundary between the electrolyte melt and gases (or in the melt) has also been proposed [12,14]. Further transport of species in the molten carbonates may occur through an oxo-Grotthuss mechanism via pyrocarbonate ions [15] or a "cogwheel" mechanism [16].

As the cathode is considered a limiting factor due to its reaction speed, many experimental studies have been conducted to modify its properties in order to improve the performance of the molten carbonate fuel cell. However, these studies were mostly accomplished by modifying the chemical composition of the cathode. There are two main objectives of chemical modifications, both surface and volumetric. First of them is extension of the lifetime of the cell by reducing the solubility of the cathode in the molten carbonate environment for example by the addition of elements such as titanium [17–19], magnesium [20,21], yttrium [22], lanthanum [23–25] or cobalt in dual [26–30] or triple systems with addition of iron [31,32]. Another approach assumes increased catalytic activity of the cathode in the oxygen reduction reaction and is realized by adding elements such as niobium [33,34], cerium [35–37] or silver [38]. There are not many reports from research on the influence of the cathode microstructure on cell performance. Nonetheless, the effect of the microstructure, and in particular pore size distribution, on the electrolyte spatial distribution [39] and the fuel cell performance [40] is experimentally confirmed, the understanding of such a relationship requires deeper insight into the electrolyte capillary action phenomenon and possible catalytic reaction mechanisms.

Numerical modeling is a useful tool to study the microstructure of the MCFC cathodes and the phenomena occurring during cell operation. Many models were developed for that purpose. The agglomerate model is the most well-known example for representing the MCFC electrodes [41]. It consists of two regions: micropores in-between agglomerates of electrode particles, completely flooded with electrolyte, and empty macropores between agglomerates. Unfortunately, the simplicity of the geometric representation render it impossible to study electrolyte filling or to include the features of realistic microstructures [42] with this model. In comparison, stochastic models (i.e. granular [43]) have been developed, that can reflect the real microstructures with a high degree of precision.

Mathematical modeling can also be applied to study the mass transport [44,45], electrolyte distribution in MCFC cathodes [46] and the cell/stack operation [47–50]. In a work [51], the macroscopic distribution of molten carbonates in MCFC electrodes was studied for various conditions (i.e. gas composition, polarization and pressures). However, this model assumed a heterogenous microstructure, which is not sufficient due to the latest reports of the role pore size distribution plays in fuel cell operation [40]. Another model developed in [52], generated a 3D cell grid representing the electrolyte distribution in the microstructure of the electrode through stochastic methods. However, this method does not take into account the real wetting of the cathode, which preserves the continuity of the fluid. That could be achieved through computational fluid dynamic (CFD) simulations.

In the present work, to address the abovementioned limitations, CFD simulations of the capillary action phenomena in molten carbonate fuel cell electrodes were performed. Tomographic images of four cathode samples from our previous studies [40] were used to represent the 3D structure of porous space for further capillary infiltration simulations. Gas-liquid equilibrium interfaces were obtained, and their characteristics were studied and compared to the results from real operational tests of MCFCs with these cathodes.

2. Materials and methods

X-ray tomographic images of four MCFC cathode samples obtained within previous studies [40] were used to create 3D models. Cathodes differed in pore size distribution thanks to the use of porogens with different particle sizes. The reference cathode (indicated as Ref), without porogen addition, showed a relatively homogenous pore size. In this case pores were formed due to the removal of the polymeric binder during the firing process [53]. Other cathodes were fabricated with the use of starch (denoted as P1) with a particle size in the range of 5–25 μm and polyvinyl butyral (P2) with a particle size up to 70 μm, or both of porogens (P1+P2). The fractions of the main tape casting slurry components are listed in Table 1. Our previous studies [43,53] have shown that using electrodes with a porosity in the range of 50 ÷ 60% and mean pore diameter 5 ÷ 15 μm assures a relatively high specific surface area. Due to the fact that the cathode oxidizes in-situ from nickel to nickel oxide preferably the initial green material porosity should be 5% higher. The fraction of porogens were adjusted to obtain desirable porosity. It should be noted however that due to a technological barrier, where the larger addition of porogen P1 (starch) resulted in brittleness of the tape, we decided to keep the maximum fraction of P1 in all the samples at 7.5 wt%.

Models of the pore space were created based on the 3D images from micro-computed tomography in Avizo software. Representative regions [43] of dimension 100 × 100 × 100μm were subtracted from the larger tomographic data. Inversion of the data was performed to select the pore

Table 1
Composition of the slurries for casting of green tapes.

Sample	Nickel powder, wt %	Liquid phase wt %	Porogen P1, wt %	Porogen P2, wt %	Mean pore size [μm]
Ref	55.0	45	0	0	6.7
P1	55.0	37.5	7.5	0	8.7
P2	55.0	35.0	0	10.0	14.6
P1+P2	55.0	32.5	7.5	5.0	15.9

space and after that an STL (stereolithography format) surface was generated. Next, the surface models were exported to Ansys ICEM CFD software to generate the volumetric mesh for CFD calculations. A mesh convergence study, performed for the sample denoted as Ref (with smallest pore sizes) revealed that a mesh size of 2 μm is an optimal value for accuracy versus the time need for the numerical calculations.

The simulation of the capillary action phenomenon was performed in Ansys Fluent. The Volume of Fluid (VOF) method was used as a multi-phase interface tracking technique. Gravitational acceleration was set in the Y-direction with the standard value of 9.81 m s^{-2}. Molten carbonate properties were set according to data from literature [54]: density of 1.95 g cm^{-3}, surface tension of 0.208 N m^{-1}, and nickel-carbonate contact angle of 5°. The wall adhesion option was enabled, so that the contact angle on the material surface could be set. Implicit Body Force correction in the momentum equation was included, due to the existence of large body forces (gravity and surface tension forces) in the phenomenon studied. The Fractional Step scheme of pressure velocity-coupling was chosen to improve the speed of the calculations. The Non-Iterative Time-Advancement Scheme for solving the transport equations was also enabled to speed up the transient simulation. Improving speed of calculations was necessary because an exceedingly small element size produced an exceedingly small timestep of 10^{-8} s, due to the Courant Number limitation. The initial level of molten carbonates in the pore space was set to 30 μm in the lower part of the model. An Outflow condition was set on the upper end of the simulation domain. The lower end and sides of the simulation domain were set as walls with no contact angle set, to ensure a constant volume of liquid and rising of the carbonates only due to the capillary forces. Wall with a No Slip condition and a static contact angle were set on the surfaces representing the material. The simulations were stopped when the sum of velocities for all phases approached a constant value.

After the simulations, volumes with the value of the volume fraction of molten carbonates above 0.5 (electrolyte) and below 0.5 (gases), were extracted and converted to STL files in ANSYS CFD Post. The triple phase boundary density (TPBD) and electrolyte specific surface area (specific surface area of the interface between electrolyte and pore – $S_V^{E/P}$) were calculated by the methods described in [39]. These parameters were correlated with the maximum power density of the cathodes measured experimentally in [40].

3. Results and discussion

Our previous experimental investigations [40] of cathode materials (not oxidized and without presence of electrolyte) have shown that for 10 wt% of porogen P2, larger pores are not fully connected. On the other hand addition of 7.5% of much smaller porogen P1 results in smaller but more evenly distributed pores, which brings higher continuity of pore network. Unfortunately, smaller pores formed due to addition of porogen P1 are partly infiltrated by the electrolyte (due to capillary action phenomenon) and the open space for gas transport is reduced. In the case of P1+P2 larger pores (introduced by addition of porogen P2) are connected by smaller channels introduced by addition of porogen P1.

The model developed within this study allowed for the investigation of the dynamics of the infiltration of cathodes by the electrolyte. In Fig. 1, the 3D distribution of the electrolyte is presented for the cathodes that produced the highest discrepancy in fuel cell maximum power density. The results show that small pores are fully infiltrated by the electrolyte and the larger ones are open (see Fig. 1 a,b). Consequently, the presence of large open pores covered by the electrolyte film enhances the gas transport and increases the specific surface area of the electrolyte/gas interface (see Fig. 1 c,d).

Quantitative analysis enabled investigating the microstructure in more detail. Fig. 2, shows the triple phase boundary density (TPBD) and the electrolyte specific surface area (ESSA) at the gas-liquid interface. It can be noticed that the addition of porogen particles slightly decreases TPBD, especially for samples with a larger porogen addition (P1+P2, P2). The reference sample with no porogen addition had the highest TPBD. This can be attributed to the presence of larger pores in the pore

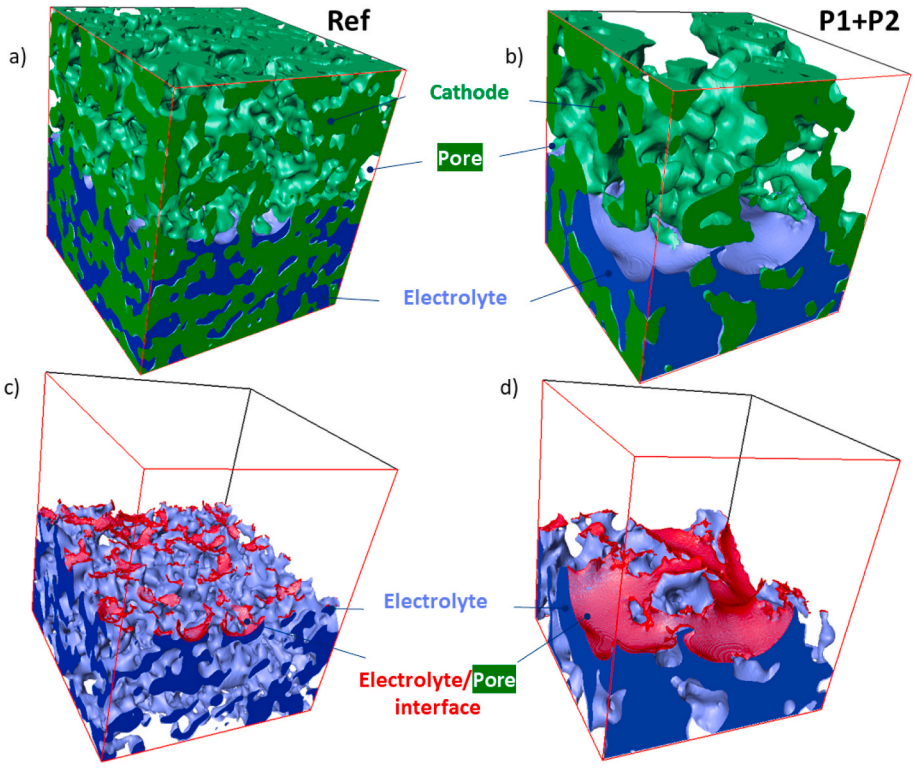

Fig. 1. Visualizations of electrolyte distribution after simulation for reference a), and mixed porogens b) samples. Figures c) and d) present only electrolyte distribution within material for the same samples.

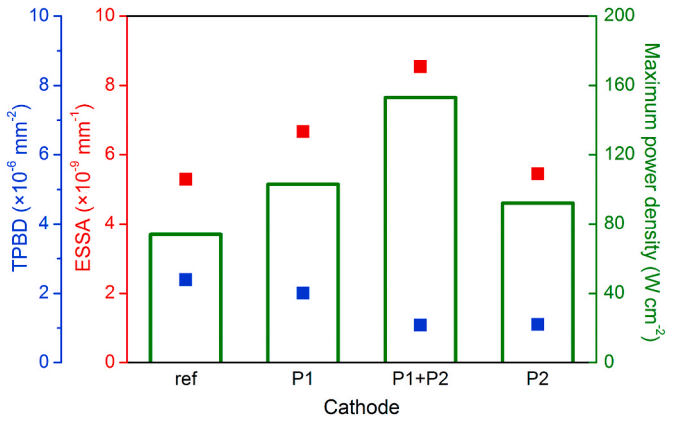

Fig. 2. The results of triple phase boundary density (TPBD) and electrolyte specific surface area (ESSA) compared with the results of fuel cell performance.

space, which massively increases the surface area of the gas-liquid interface. The highest value of surface area of the gas-liquid interface was obtained for the sample P1+P2, which also exhibited the highest porosity – 65,1%. However, porosity was not the only determining factor for the molten carbonate surface area. Sample P1 had a higher surface area than sample P2, despite lower porosity – 50.3 and 58.1 respectively. Additionally, there was no correlation with the mean pore size values presented in [40]. This leads to the conclusion, that heterogeneity of the spatial pore distribution [40] is also important for the capillary action phenomenon in the porous structure of MCFC electrodes and the electrolyte spatial distribution. Additionally, it can be observed, that the bigger pores are not fully flooded – a thin film of electrolyte forms on the edges. This is consistent with results from other studies [55], where the cathode microstructure flooding was observed in situ.

In Fig. 2, the specific surface area of the gas-liquid interface for all cathodes was corelated with the maximum power density obtained by the fuel cells operated with the cathodes studied in our previous work [40]. The single-cell test was performed for all cathode samples with an effective electrode area of 20.25 cm^2 $(H_2)80/(CO_2)20\%$ as the fuel gas and $(Air)70/(CO_2)30\%$ as the oxidant gas were fed during the test in 650 °C. Information regarding full experimental set-up can be found in [40]. The results obtained within this study suggest that the cathode reaction rate may be also determined by the specific surface area of the gas-electrolyte interface, and not only by TPBD as it is usually proposed.

During the cathode reaction, a TPB formed between the surface of the lithiated nickel oxide cathode, molten lithium-potassium carbonate electrolyte, and pore space with CO_2 and O_2 gasses serving as active sites for the transformation into carbonate ions CO_3^{2-} but also as a source of superoxide ions - active forms of oxygen. Molecular oxygen is activated due to the charge transfer from the electron-rich surface of the cathode and desorbed with a near-zero energy barrier [8]. Desorbed superoxide ions easily infiltrate the electrolyte due to their higher solubility in molten carbonates [56,57] than the molecular oxygen [58]. Carbon dioxide is also highly soluble in molten carbonates [15]. Thus, the coupling between CO_2 with the active oxygen may be possible in the melt and further transformation may occur into other species involved in the charge or ion transport in molten carbonates (e.g. through an oxo-Grotthuss or a “cogwheel” mechanism). Despite that the oxygen reduction is considered as the slowest process in the cathode reaction (rate determining step), at the high MCFC operating temperature, 650 °C, the cathode provides sufficient catalytic activity for oxygen activation. Therefore, even if the total TPB length is decreasing, the increment of maximum power density stays in close correlation to the surface area of the electrolyte-gas interface through which carbon dioxide can infiltrate the melt, and subsequently be coupled with the active oxygen species present or engaged in the ion transport mechanisms.

However, the solubility of oxygen in molten carbonates is one order of magnitude lower than for carbon dioxide. This fact, coupled with the observation of the thin film in larger pores, can explain the rise of the maximum power density by the additional reaction mechanism. The decrease of the diffusion path to the electrode surface enables faster oxygen transport to the reduction zone and its adsorption on a larger cathodic surface area, despite low solubility. That would greatly increase the reduction rate of oxygen, which is considered the rate determining step for the overall cathodic reaction. A similar effect was observed in the work [55], where the thin film area was identified as the region with the highest reaction activity. This mechanism was postulated in [59], and is presented in Fig. 3. It assumes, that both oxygen and carbon dioxide diffuses into the melt. Dissolved oxygen is transported through thin layer of molten carbonates to the electrode interface, where it is adsorbed and reduced. The oxide ion O^{2-} can diffuse into the melt, and together with carbon dioxide can form carbonate ion.

4. Conclusions

In summation, we developed a model of capillary action for a porous MCFC cathode based on 3D structures generated from micro-computed X-ray tomography (μ-XCT), and volume of fluid (VOF) computations. Based on the results of simulations, we are able to visualize the spatial distribution of molten carbonate electrolyte in the pore space of cathodes with varying pore size distribution, emphasizing particularly the area of the electrolyte-gas interface (which can be calculated). Pore size distribution in the cathode strongly determines the area of the electrolyte-gas interface (hereinafter electrolyte specific surface area, ESSA) and the density of active sites (triple-phase boundary density, TPBD) for the electrochemical reactions, as the qualitative analysis showed. Smaller pores are fully flooded by the electrolyte but larger ones, with their surfaces covered by a thin film of electrolyte, remain open for gas transport. Therefore, the highest electrolyte specific surface area (ESSA) and the lowest triple-phase boundary density (TPBD), and the inverse relationships in the mono-modal cathodes (P1, P2) were observed in the cathode with the multi-modal (P1+P2) pore size distribution. The multi-modal cathode (P1+P2) reached substantially higher maximum power density, 153 mW cm^{-2}, comparing to the mono-modal counterparts P1 and P2 – 103 and 92 mW cm^{-2} respectively. Electrolyte specific surface area (ESSA) stays in close correlation with the maximum power density obtained by the cells operated with cathodes analyzed, and it is calculated as 8.54, 6.66, and 5.45×10^{-6} mm^{-1} for P1+P2, P1 and P2 cathode respectively. We have, thus, elucidated the importance of the role of the thin electrolyte film as a region providing the pathway for oxygen reduction complementary to the commonly postulated TPB mechanism (predominant in mono-modal cathodes). Especially that TPBD decreases almost two times when the fraction of bigger pores is introduced to the cathode, i.e. in P1+P2 and P2, We have also proposed the interpretation of the possible mechanism of the oxygen reduction with the presence of thin electrolyte film. Despite low solubility of oxygen in molten carbonates, it may be transported more efficiently through the thin electrolyte film toward the surface of the cathode and reduced thereon. Thus, the production rate of the active forms of oxygen is increased significantly what is crucial for further reaction with carbon dioxide toward formation of carbonate ions (charge carriers). Based on the results, it may be postulated, that the oxygen reduction, as the rate determining step in the MCFC cathode reaction, is governed not only by the complex chemistry and charge transfer issues, but also by the accessibility of active sites at the cathode surface which can be facilitated by proper design of the cathode microstructure (pore size variation).

CRediT authorship contribution statement

Samih Haj Ibrahim: Software, Methodology, Investigation, Writing - original draft. **Tomasz Wejrzanowski:** Conceptualization,

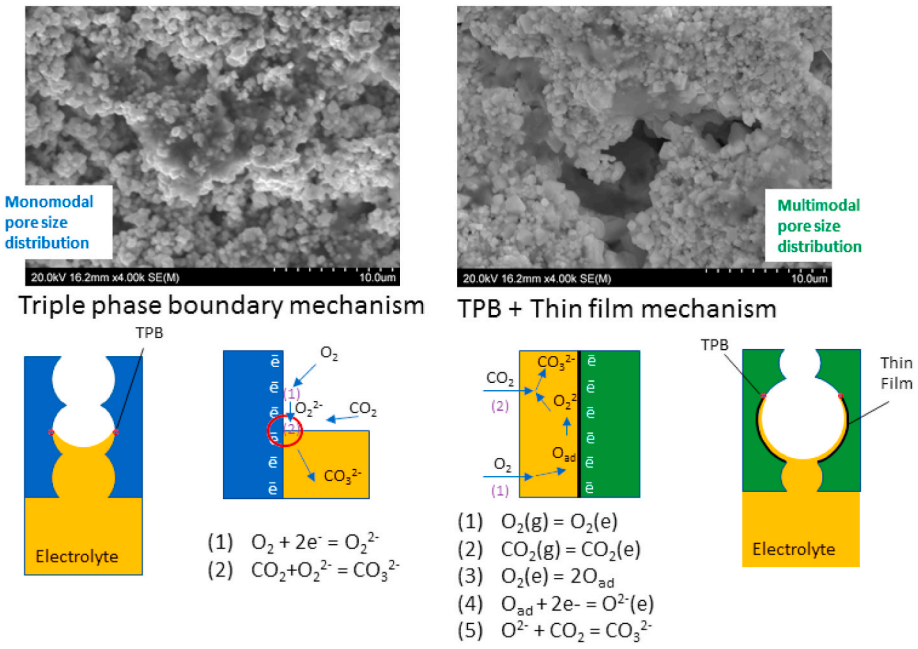

Fig. 3. Additional reaction mechanism explaining the better performance for cathodes with bigger pores.

Supervision, Writing - original draft. **Pawel Sobczak:** Software, Investigation, Methodology. **Karol Cwieka:** Resources, Writing - original draft. **Aleksandra Lysik:** Visualization, Writing - original draft. **Jakub Skibinski:** Methodology, Validation. **Graeme John Oliver:** Validation, Writing - review & editing.

Declaration of competing interest

The authors declare that they have no known competing financial interests or personal relationships that could have appeared to influence the work reported in this paper.

Acknowledgement

This work was financially supported by the Polish National Science Centre in the framework of the PRELUDIUM research project (Grant No. 2017/27/N/ST8/02772).

References

[1] T. Elmer, M. Worall, S. Wu, S.B. Riffat, Fuel cell technology for domestic built environment applications: state of-the-art review, Renew. Sustain. Energy Rev. 42 (2015) 913–931, https://doi.org/10.1016/j.rser.2014.10.080.
[2] A. Kulkarni, S. Giddey, Materials issues and recent developments in molten carbonate fuel cells, J. Solid State Electrochem. 16 (2012) 3123–3146, https://doi.org/10.1007/s10008-012-1771-y.
[3] P.E. Dodds, I. Staffell, A.D. Hawkes, F. Li, P. Grünewald, W. McDowall, P. Ekins, Hydrogen and fuel cell technologies for heating: a review, Int. J. Hydrogen Energy 40 (2015) 2065–2083, https://doi.org/10.1016/j.ijhydene.2014.11.059.
[4] T. Watanabe, Y. Izaki, Y. Mugikura, H. Morita, M. Yoshikawa, M. Kawase, F. Yoshiba, K. Asano, Applicability of molten carbonate fuel cells to various fuels, J. Power Sources 160 (2006) 868–871, https://doi.org/10.1016/j.jpowsour.2006.06.058.
[5] A.L. Dicks, Molten carbonate fuel cells, Curr. Opin. Solid State Mater. Sci. 8 (2004) 3113–3138, https://doi.org/10.1016/j.cossms.2004.12.005.
[6] T. Wejrzanowski, K. Cwieka, J. Skibinski, A. Lysik, S. Haj Ibrahim, J. Milewski, W. Xing, Microstructure driven design of porous electrodes for molten carbonate fuel cell application: recent progress, Int. J. Hydrogen Energy 45 (2020) 25719–25732.
[7] J. Molenda, J. Kupecki, R. Baron, M. Blesznowski, G. Brus, T. Brylewski, M. Bucko, J. Chmielowiec, K. Cwieka, M. Gazda, A. Gil, P. Jasinski, Z. Jaworski, J. Karczewski, M. Kawalec, R. Kluczowski, M. Krauz, F. Krok, B. Lukasik, M. Malys, A. Mazur, A. Mielewczyk-Gryn, J. Milewski, S. Molin, G. Mordarski, M. Mosialek, K. Motylinski, E.N. Naumovich, P. Nowak, G. Pasciak, P. Pianko-Oprych, D. Pomykalska, M. Rekas, A. Sciazko, K. Swierczek, J. Szmyd, S. Wachowski, T. Wejrzanowski, W. Wrobel, K. Zagorski, W. Zajac, A. Zurawska, Status report on high temperature fuel cells in Poland – recent advances and achievements, Int. J. Hydrogen Energy 42 (2017) 4366–4403, https://doi.org/10.1016/j.ijhydene.2016.12.087.
[8] K. Czelej, K. Cwieka, J.C. Colmenares, K.J. Kurzydlowski, Atomistic insight into the electrode reaction mechanism of the cathode in molten carbonate fuel cells, J. Mater. Chem. A. 5 (2017), https://doi.org/10.1039/c7ta02011b.
[9] K. Czelej, K. Cwieka, J.C. Colmenares, K.J. Kurzydlowski, Catalytic activity of NiO cathode in molten carbonate fuel cells, Appl. Catal. B Environ. 222 (2018), https://doi.org/10.1016/j.apcatb.2017.10.003.
[10] K. Czelej, K. Cwieka, T. Wejrzanowski, P. Spiewak, K.J. Kurzydlowski, Decomposition of activated CO_2 species on Ni(110): role of surface diffusion in the reaction mechanism, Catal. Commun. 74 (2016) 65–70.
[11] C.-Y. Yuh, J.R. Selman, The polarization of molten carbonate fuel cell electrodes, J. Electrochem. Soc. 138 (1991) 3649–3656, https://doi.org/10.1149/1.2085474.
[12] K. Hemmes, J.R. Selman, O_2-reduction at high temperature: MCFC, in: W. Vielstich, H.A. Gasteiger, A. Lamm, H. Yokokawa (Eds.), Handb. Fuel Cells – Fundam. Technol. Appl, John Wiley & Sons, Inc., 2010.
[13] X. Lei, K. Haines, K. Huang, C. Qin, DFT study of oxygen dissociation in molten carbonate, J. Phys. Chem. 119 (2015) 8806–8812, https://doi.org/10.1021/acs.jpca.5b06527.
[14] A.J. Appleby, S.B. Nicholson, Reduction of oxygen in alkali carbonate melts, J. Electroanal. Chem. Interfacial Electrochem. 83 (1977) 309–328, https://doi.org/10.1016/S0022-0728(77)80176-9.
[15] D. Corradini, F.-X. Coudert, R. Vuilleumier, Carbon dioxide transport in molten calcium carbonate occurs through an oxo-Grotthuss mechanism via a pyrocarbonate anion, Nat. Chem. 8 (2016) 454–460, https://doi.org/10.1038/nchem.2450.
[16] X. Lei, K. Haines, K. Huang, C. Qin, Density functional theory study of oxygen migration in molten carbonate, J. Power Sources 305 (2016) 161–166, https://doi.org/10.1016/j.jpowsour.2015.11.095.
[17] M.Z. Hong, H.S. Lee, M.H. Kim, E.J. Park, H.W. Ha, K. Kim, TiO2-coated Ni powder as a new cathode material for molten carbonate fuel cells, J. Power Sources 156 (2006) 158–165, https://doi.org/10.1016/j.jpowsour.2005.03.236.
[18] A. Meléndez-Ceballos, S.M. Fernández-Valverde, C. Barrera-Díaz, V. Albin, V. Lair, A. Ringuedé, M. Cassir, TiO2 protective coating processed by Atomic Layer Deposition for the improvement of MCFC cathode, Int. J. Hydrogen Energy 38 (2013) 13443–13452, https://doi.org/10.1016/j.ijhydene.2013.07.083.
[19] A. Meléndez-Ceballos, V. Albin, A. Ringuedé, S.M. Fernández-Valverde, M. Cassir, Electrochemical behavior of Mx-1Ox(M = Ti, Ce and Co) ultra-thin protective layers for MCFC cathode, Int. J. Hydrogen Energy 39 (2014) 12233–12241, https://doi.org/10.1016/j.ijhydene.2014.03.213.
[20] K. Mustafa, M. Anwar, M. Akmal Rana, Z.S. Khan, Development of cobalt doped lithiated NiO nano-composites and hot corrosion testing of LiAlO matrices for molten carbonate fuel cell (MCFC) applications, Mater. Chem. Phys. 164 (2015) 198–205, https://doi.org/10.1016/j.matchemphys.2015.08.044.
[21] H. Okawa, J.H. Lee, T. Hotta, S. Ohara, S. Takahashi, T. Shibahashi, Y. Yamamasu, Performance of NiO/MgFe2O4composite cathode for a molten carbonate fuel cell, J. Power Sources 131 (2004) 251–255, https://doi.org/10.1016/j.jpowsour.2003.11.092.
[22] B. Huang, X. feng Ye, S. rong Wang, Q. chun Yu, H. wen Nie, Q. Hu, J. Shi, K. ao Hu, T. lian Wen, Electrochemical performance of Y2O3/NiO cathode in the molten

Li0.62/K0.38 carbonates eutectics, Mater. Res. Bull. 41 (2006) 1935–1948, https://doi.org/10.1016/j.materresbull.2006.03.007.
[23] K. Matsuzawa, G. Tatezawa, Y. Matsuda, S. Mitsushima, N. Kamiya, K. Ota, Effects of rare-earth additives in Li/Na eutectic carbonate for decreasing the solubility of NiO, J. Electrochem. Soc. 152 (2005) A1116, https://doi.org/10.1149/1.1904985.
[24] K. ichiro Ota, Y. Matsuda, K. Matsuzawa, S. Mitsushima, N. Kamiya, Effect of rare earth oxides for improvement of MCFC, J. Power Sources 160 (2006) 811–815, https://doi.org/10.1016/j.jpowsour.2006.04.055.
[25] K. Matsuzawa, T. Mizusaki, S. Mitsushima, N. Kamiya, K.I. Ota, The effect of La oxide additive on the solubility of NiO in molten carbonates, J. Power Sources 140 (2005) 258–263, https://doi.org/10.1016/j.jpowsour.2004.08.041.
[26] P. Ganesan, H. Colon, B. Haran, R. White, B.N. Popov, Study of cobalt-doped lithium-nickel oxides as cathodes for MCFC, J. Power Sources 111 (2002) 109–120, https://doi.org/10.1016/S0378-7753(02)00301-4.
[27] M.J. Escudero, L. Mendoza, M. Cassir, T. Gonzalez, L. Daza, Porous nickel MCFC cathode coated by potentiostatically deposited cobalt oxide. II. Structural and morphological behavior in molten carbonate, J. Power Sources 160 (2006) 775–781, https://doi.org/10.1016/j.jpowsour.2006.04.056.
[28] E. Simonetti, R. Lo Presti, Characterization of Ni porous electrode covered by a thin film of LiMg0.05Co0.95O2, J. Power Sources 160 (2006) 816–820, https://doi.org/10.1016/j.jpowsour.2006.04.114.
[29] H. Lee, M. Hong, S. Bae, H. Lee, E. Park, K. Kim, A novel approach to preparing nano-size Co3O4-coated Ni powder by the Pechini method for MCFC cathodes, J. Mater. Chem. 13 (2003) 2626–2632, https://doi.org/10.1039/b303980c.
[30] Y.S. Kim, C.-W. Yi, H.S. Choi, K. Kim, Modification of Ni-based cathode material for molten carbonate fuel cells using CO3O4, J. Power Sources 196 (2011) 1886–1893, https://doi.org/10.1016/j.jpowsour.2010.08.086.
[31] A. Ringuedé, A. Wijayasinghe, V. Albin, C. Lagergren, M. Cassir, B. Bergman, Solubility and electrochemical studies of LiFeO2-LiCoO2-NiO materials for the MCFC cathode application, J. Power Sources 160 (2006) 789–795, https://doi.org/10.1016/j.jpowsour.2006.04.136.
[32] A. Wijayasinghe, C. Lagergren, B. Bergman, New cathode materials for molten carbonate fuel cells, Fuel Cell. 2 (2002) 181–188, https://doi.org/10.1002/fuce.200290019.
[33] B. Fang, H. Chen, A new candidate material for molten carbonate fuel cell cathodes, J. Electroanal. Chem. 501 (2001) 128–131, https://doi.org/10.1016/S0022-0728(01)00379-5.
[34] B. Fang, C. Zhou, X. Liu, S. Duan, Performance of a novel Ni/Nb cathode material for molten carbonate fuel cells (MCFC), J. Appl. Electrochem. 31 (2001) 201–205, https://doi.org/10.1023/A:1004130520415.
[35] L. Daza, C.M. Rangel, J. Baranda, M.T. Casais, M.J. Martínez, J.A. Alonso, Modified nickel oxides as cathode materials for MCFC, J. Power Sources 86 (2000) 329–333, https://doi.org/10.1016/S0378-7753(99)00499-1.
[36] M.J. Escudero, T. Rodrigo, L. Daza, Molten carbonate fuel cell cathodes: improvement of the electrocatalytic activity, Catal. Today 107–108 (2005) 377–387, https://doi.org/10.1016/j.cattod.2005.07.097.
[37] A. Meléndez-Ceballos, V. Albin, S.M. Fernández-Valverde, A. Ringuedé, M. Cassir, Electrochemical properties of Atomic layer deposition processed CeO2as a protective layer for the molten carbonate fuel cell cathode, Electrochim. Acta 140 (2014) 174–181, https://doi.org/10.1016/j.electacta.2014.05.025.
[38] A. Lysik, T. Wejrzanowski, K. Cwieka, J. Skibinski, J. Milewski, F.M.B. Marques, T. Norby, Silver Coated Cathode for Molten Carbonate Fuel Cells, 2020.
[39] T. Wejrzanowski, J. Gluch, S. Haj Ibrahim, K. Cwieka, J. Milewski, E. Zschech, Characterization of spatial distribution of electrolyte in molten carbonate fuel cell cathodes, Adv. Eng. Mater. 20 (2018) 1700909, https://doi.org/10.1002/adem.201700909.
[40] T. Wejrzanowski, S. Haj Ibrahim, K. Cwieka, M. Loeffler, J. Milewski, E. Zschech, C.-G. Lee, Multi-modal porous microstructure for high temperature fuel cell application, J. Power Sources 373 (2018) 85–94, https://doi.org/10.1016/J.JPOWSOUR.2017.11.009.
[41] J.A. Prins-Jansen, K. Hemmes, J.H.W. de Wit, An extensive treatment of the agglomerate model for porous electrodes in molten carbonate fuel cells I. Qualitative analysis of the steady state model, Electrochim. Acta 42 (1997) 3585–3600, https://doi.org/10.1016/S0013-4686(97)00032-7.
[42] E. Fontes, C. Lagergren, D. Simonsson, Mathematical modelling of the MCFC cathode, Electrochim. Acta 38 (1993) 2669–2682, https://doi.org/10.1016/0013-4686(93)85085-D.
[43] S. Haj Ibrahim, M. Neumann, F. Klingner, V. Schmidt, T. Wejrzanowski, Analysis of the 3D microstructure of tape-cast open-porous materials via a combination of experiments and modeling, Mater. Des. 133 (2017) 216–223, https://doi.org/10.1016/j.matdes.2017.07.058.
[44] A. Bodén, G. Lindbergh, A model for mass transport of molten alkali carbonate mixtures applied to the MCFC, J. Electrochem. Soc. 153 (2006) A2111, https://doi.org/10.1149/1.2338653.
[45] S. Haj Ibrahim, J. Skibinski, G.J. Oliver, T. Wejrzanowski, Microstructure effect on the permeability of the tape-cast open-porous materials, Mater. Des. 167 (2019) 107639, https://doi.org/10.1016/j.matdes.2019.107639.
[46] E. Fontes, M. Fontes, D. Simonsson, A heterogeneous model for the MCFC cathode, Electrochim. Acta 40 (1995) 1641–1651, https://doi.org/10.1016/0013-4686(95)00076-Q.
[47] A. Szczęśniak, J. Milewski, Ł. Szabłowski, W. Bujalski, O. Dybiński, Dynamic model of a molten carbonate fuel cell 1 kW stack, Energy 200 (2020), https://doi.org/10.1016/j.energy.2020.117442.
[48] J. Milewski, A. Szczęśniak, Ł. Szabłowski, O. Dybiński, A. Miller, Artificial neural network model of molten carbonate fuel cells: validation on experimental data, Int. J. Energy Res. 43 (2019) 6740–6761, https://doi.org/10.1002/er.4608.
[49] E. Audasso, S. Nam, E. Arato, B. Bosio, Preliminary model and validation of molten carbonate fuel cell kinetics under sulphur poisoning, J. Power Sources 352 (2017) 216–225, https://doi.org/10.1016/j.jpowsour.2017.03.091.
[50] C.C. Chen, J.R. Selman, Anode modeling of a molten-carbonate based direct carbon fuel cell, J. Power Sources 353 (2017) 312–322, https://doi.org/10.1016/j.jpowsour.2017.03.078.
[51] M. Kawase, Y. Mugikura, T. Watanabe, An electrolyte distribution model in consideration of the electrode wetting in the molten carbonate fuel cell, J. Electrochem. Soc. 147 (2000) 854, https://doi.org/10.1149/1.1393282.
[52] S.-G. Hong, J.R. Selman, A stochastic structure model for liquid-electrolyte fuel cell electrodes, with special application to MCFCs, J. Electrochem. Soc. 151 (2004) A739, https://doi.org/10.1149/1.1695381.
[53] K. Cwieka, S. Haj Ibrahim, J. Milewski, T. Wejrzanowski, Effect of anode porosity on the performance of molten carbonate fuel cell, J. Power Technol. 98 (2018) 228–237.
[54] A.T. Ward, G.J. Janz, Molten carbonate electrolytes: electrical conductance, density and surface tension of binary and ternary mixtures, Electrochim. Acta 10 (1965) 849–857, https://doi.org/10.1016/0013-4686(65)80048-2.
[55] M. Kawase, K. Asano, H. Murata, Y. Mugikura, T. Watanabe, Y. Ito, In situ microobservation of the cathode in molten carbonate fuel cells, J. Appl. Electrochem. 32 (2002) 185–191, https://doi.org/10.1023/A:1014773014639.
[56] A.J. Appleby, C. Van Drunen, Solubilities of oxygen and carbon monoxide in carbonate melts, J. Electrochem. Soc. 127 (1980) 1655, https://doi.org/10.1149/1.2129975.
[57] M. Cassir, G. Moutiers, J. Devynck, Stability and characterization of oxygen species in alkali molten carbonate: a thermodynamic and electrochemical approach, J. Electrochem. Soc. 140 (1993) 3114, https://doi.org/10.1149/1.2220995.
[58] S. Frangini, S. Scaccia, The role of foreign cations in enhancing the oxygen solubility properties of alkali molten carbonate systems: brief survey of existing data and new research results, Int. J. Hydrogen Energy 39 (2014) 12266–12272, https://doi.org/10.1016/j.ijhydene.2014.02.042.
[59] R.C. Makkus, K. Hemmes, J.H.W. de Wit, A comparative study of NiO (Li), $LiFeO_2$, and $LiCoO_2$ porous cathodes for molten carbonate fuel cells, J. Electrochem. Soc. 141 (2019) 3429–3438, https://doi.org/10.1149/1.2059349.